UNIVERSITY OF CALIFORNIA SAN DIEGO

Arid1a Loss in Macrophages Upregulates Expression of PD-L1 and Increases Efficacy of PD-L1 Checkpoint Blockade

A thesis submitted in partial satisfaction of the requirements
for the degree of Master of Science

in

Biology

by

Katherine M. Nguyen

Committee in charge:

Professor Diana Hargreaves, Chair
Professor Enfu Hui, Co-Chair
Professor Ananda Goldrath

2022

The Thesis of Katherine M. Nguyen is approved, and is acceptable in quality and Form of on microfilm and electronically.

University of California San Diego

2022

DEDICATION

I would like to dedicate my thesis to my mother, family abroad, Dr. Sanjai Gupta, and friends for all the love and support.

TABLE OF CONTENTS

LIST OF FIGURES

LIST OF TABLES

LIST OF ABBREVIATIONS

ARID1A	AT-Rich Interaction Domain 1A
BMDM	Bone marrow derived macrophage
DMEM	Dulbecco's modified eagles media
FACS	Fluorescent activated cell sorting
FBS	Fetal bovine serum
IFNγ	Interferon gamma
IFNβ	Interferon gamma
IL-6	Interleukin 6
KO	Knockout
M-CSF	Macrophage colony stimulating factor
PBS	Phosphate buffered saline
PD-L1	Program death ligand-1
TAM	Tumor associated macrophage
TIF	Tumor interstitial fluid
TIL	Tumor infiltrating lymphocytes
TME	Tumor microenvironment

ACKNOWLEDGEMENTS

I would first like to express my appreciation and gratitude to my PI, Diana Hargreaves, for taking a chance on me during the pandemic and welcoming me into the lab with open arms. The research opportunity, scientific knowledge, and guidance you have given me is invaluable. Next, I would like to express my deepest gratitude to Dr. Helen McRae, my mentor, for all your advice, patience, daily training, and presence. Without your willingness to take on a very new and very green trainee, none of this would have been possible. Because of your nurturing presence, my confidence in my own knowledge and execution of technical skills have grown immensely. Additionally, I would like to thank each person in the Hargreaves Lab at the Salk Institute. Our daily conversations, outings, and collaborations have truly made this last year feel like a second home. Thank you all for assisting me with any questions and creating a positive and close-knit environment. I would also like to acknowledge my thesis committee members, Enfu Hui and Ananda Goldrath for their insight.

I would also like to thank Dr. Sanjai Gupta from Irvine Valley College. You have been instrumental in my success as a student from the beginning. Never in a million years could I imagine any of this was possible. Had I never taken your class, I would not have pursued my degree nor think I was even capable of doing so. Thank you for your passion for education and most of all, your belief in my abilities. I am grateful for your continued mentorship and direction throughout the years and for the years to come.

Finally, to my mother, thank you for being my rock, sun, moon, and everything in between. This past year has been the most taxing, but you have been there every step of the way offering encouragement. You have always continually pushed me when needed and supported me in every endeavor. You have always been my biggest cheerleader and because of you I have made it to the end.

ABSTRACT OF THE THESIS

Arid1a Loss in Macrophages Upregulates Expression of PD-L1 and Increases Efficacy of PD-L1 Checkpoint Blockade

by

Katherine M. Nguyen

Master of Science in Biology

University of California San Diego, 2022

Professor Diana Hargreaves, Chair
Professor Enfu Hui, Co-Chair

Tumor associated macrophages (TAMs) are a major component in the tumor microenvironment. TAMs are associated with poor prognosis in solid tumors and promote an immunosuppressive environment, which can result from persistent inflammation. Preclinical studies suggest boosting existing immunotherapies by

reprogramming TAMs from a pro-tumor phenotype towards an anti-tumor one. To better target these TAMs, we must look at the complexes that regulate them. The BAF complex, an ATP-dependent chromatin remodeler, regulates gene expression by altering the position of nucleosomes to promote gene expression. ARID1A, a core protein subunit of cBAF plays a vital role in the epigenetic regulation of inflammatory genes and the differentiation of myeloid cells. Little is known about the effects of *Arid1a* loss in TAMs and its implications in cancer. We sought to recapitulate the effects of *Arid1a* loss on macrophages *in vitro*, investigate the mechanisms driving the associated phenotype, and assess phagocytotic function in *Arid1a*-deficient (*Arid1a*KO) TAMs. Using an *in vitro* system of bone marrow derived macrophages (BMDMs), we observed that *Arid1a*KO macrophages upregulated the inhibitory ligand PD-L1 (programmed death ligand-1) and CD86. This upregulation is both JAK1/2 and type I interferon signaling independent and operates through a cell intrinsic mechanism. Furthermore, we found that *Arid1a*KO TAMs displayed similar phagocytic capabilities to *Arid1a*-intact TAMs. Our results demonstrate that upregulation of PD-L1 and CD86 in macrophages that occurs upon *Arid1a* loss may explain enhanced response to anti-PD-L1 immunotherapy. In the future, these results can help further direct preclinical models/strategies aimed at reprogramming macrophages as a cancer therapeutic.

INTRODUCTION

1.1 Motivation

In the United States, cancer is the leading cause of death behind heart disease. In fact, the American Cancer Society predicts that approximately two million people will be diagnosed with cancer by the end of 2022. For both men and women, the highest rate of incidence and mortality can be attributed to solid cancers [30]. By acquiring mutations, these cancer cells can proliferate uninhibited by evading both cellular and immunological checkpoints [15]. Immunotherapy, one type of cancer therapeutic, is aimed at preventing further evasion of the immune system by harnessing a patient's existing immune cells to kill cancerous ones [25, 32]. Patients suffering from hematologic cancers have seen relative success with immunotherapy in recent years, however, response rates in solid cancers have not yielded equivalent responses [13, 28]. To improve immunotherapy response rates, a better understanding of the molecular interactions between cancer cells and our immune system is required [16].

1.2 Background

1.2.1 Tumor microenvironment

The tumor microenvironment (TME) is one factor that can be attributed to the poor efficacy of immunotherapy in solid cancers [13]. The TME is a heterogenous environment consisting of immune cells, cytokines, an extracellular matrix, and mechanical cues that can either promote or protect against tumorigenesis [31]. TMEs that protect against tumorigenesis are known as 'hot' TMEs, while 'cold' TMEs tend to be more pro-tumorigenic. Hot TMEs tend to respond better to immunotherapies like PD-1/PD-L1 checkpoint blockade. They typically display increased T cell infiltration, a

molecular signature of immune activation, contain the presence of anti-tumor macrophages, and contain the presence of proinflammatory cytokines. In contrast, cold TMEs are typically less responsive to immunotherapies and are often characterized by an absence or exclusion of T cells, presence of pro-tumor macrophages, and produce more immunosuppressive cytokines [7]. The recruitment of tumor associated macrophages occurs via cues in the TME and these cues can not only alter macrophage function, but also influence the ability of macrophages to infiltrate tumors [1, 6].

1.2.2 Tumor associated macrophages

Like the TME, tumor associated macrophages (TAMs) are classified as either anti-tumorigenic or pro-tumorigenic. Anti-tumorigenic TAMs, also known as M1-like TAMs, can be induced by pro-inflammatory cytokines like IFNγ and TNFα. Once activated these M1-like TAMs will continue to promote a hot TME by secreting pro-inflammatory cytokines like TNFα, IL-6, Type I IFN, etc. In contrast, M2-like TAMs often secrete anti-inflammatory cytokines like TGFβ, IL-10, etc. M2-like TAMs promote tumor progression and can be induced through immunosuppressive cytokines like TGFβ, IL-4, IL-10, etc. [6, 27, 29]. In fact, infiltration of primarily M2-like TAMs in solid cancer often indicates a much poorer prognosis than those with a high infiltration of M1-like TAMs [1]. TAMs can regulate and mediate tumor immunity in a myriad of ways. They can influence the TME by secreting cytokines, enabling cytotoxic T lymphocyte (CTL) function, and phagocytose tumor cells. A recent study has also indicated that efferocytosis by TAMs leads to immune tolerance, and that blocking it may increase immune activation [35].

To augment existing immunotherapies, current research is aimed at targeting TAMs to enhance immune activation functions. Current strategies involve either depleting TAMs or re-programming them from M2-like to M1-like macrophages [5-6]. However, we must gain a better understanding of the molecular pathways regulating macrophages to not only effectively target these TAMs, but also identify optimal therapies [6].

1.2.4 cBAF complex

One complex shown to regulate chromatin expression in macrophages is the BAF complex [24]. The BAF complex is a multi-subunit ATP-dependent nucleosome remodeling complex. The complex regulates gene expression by altering the position of nucleosomes to expose binding sites and promote gene expression. For example, the cBAF or canonical BAF complex, has been implicated in the regulation of inflammatory gene expression [8, 10]. Research has also demonstrated that loss of BAF45A, a protein subunit of cBAF, results in a decrease of myeloid progenitors [18]. Like BAF45A, ARID1A has also been found to be indispensable for differentiation of myeloid cell lineage [14]. These studies all indicate the crucial role the cBAF complex plays in the regulation and differentiation of myeloid cells, as well as inflammatory gene expression. My thesis aims to explore the epigenetic role of ARID1A, a core protein subunit of cBAF, on macrophages.

1.3 Preliminary data

Previously, preliminary data from the Hargreaves lab indicated that *Arid1a* loss in TAMs resulted in an M1-like transcriptional signature *in vivo*. Additionally, RNAseq data

from the lab indicated the Hallmark Interferon response as a top pathway. Based on those results, the Hargreaves lab specifically analyzed interferon stimulated genes using RNAseq. The RNAseq revealed a multitude of genes like *Cd86* and *Cd274* (or PD-L1) were upregulated in *Arid1a*-deficient (*Arid1a*KO) TAMs (Figure 1A). PD-L1 is an inhibitory ligand and interaction between its receptors (PD-1) is the target of multiple immunotherapies. Because of this, the Hargreaves lab sought to specifically verify if upregulation of the gene *Cd274* also occurred at the protein level. Indeed, PD-L1 displayed a significant increase in *Arid1a*KO TAMS when compared to *Arid1a*-intact TAMs. These results indicate that in *Arid1a*KO TAMs PD-L1 is upregulated at both the RNA and protein level (Figure 1A-B).

Current research indicates that inhibition of PD-L1 on host cells, like macrophages, is important for the efficacy of anti-PD-L1 therapy [21]. Therefore, we hypothesized that upregulation of PD-L1 on *Arid1a*-deficient macrophages would render them more sensitive to anti-PD-L1 therapy. During my time as an undergraduate researcher, I assisted with experiments to test this hypothesis. As expected for the partially responsive MC38 model, anti-PD-L1-treated controls displayed approximately a 40% average reduction in tumor burden compared to isotype-treated controls. Similarly, anti-PD-L1-treated *Arid1a*-deficient mice displayed approximately a 46% reduction in tumor burden compared to isotype-treated *Arid1a*-deficient mice. When comparing between the isotype-treated control and isotype-treated *Arid1a*KO mice, our knockout mice exhibited approximately a 25% average decrease in tumor volume. When comparing between the anti-PD-L1-treated control and *Arid1a*KO mice, a similar effect can be observed. There, the *Arid1a*KO mice have a 30% average decrease in tumor

volume (Figure 2). Overall, these results indicate that loss of *Arid1a* enhances the response of anti-PD-L1 therapy under the MC38 tumor model.

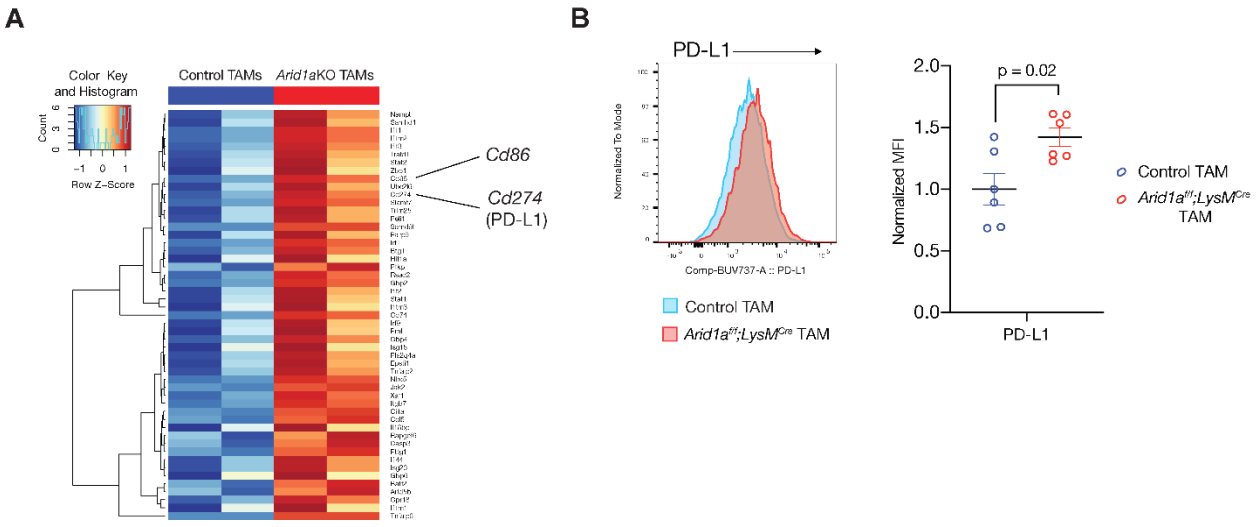

Figure 1. Arid1a-deficient macrophage tumor associated macrophages (TAMs) upregulated PD-L1.

MC38 tumors were grown in untreated control (n=15) or *Arid1a*$^{f/f}$ *LysM*^{Cre}, *Arid1a*KO, (n=11) mice. Tumor associated macrophages (TAMs) were isolated using flow sorting at day 21 and processed for transcriptional profiling using RNA-sequencing. Analysis using the Hallmark pathways from the Molecular Signatures Database (MsigDB) through the Gene Set Enrichment Analysis (GSEA) software revealed several upregulated (red) and downregulated (blue) pathways. **A)** Heatmap depicting the union of genes upregulated in the IFNγ and IFNα-stimulated gene pathways, with *CD86* and *CD274* highlighted. **B)** Cell surface expression of PD-L1 protein by flow cytometry displayed as a representative histogram and quantified using median fluorescence intensity (MFI). All data were normalized to the control value within each experiment. Data here is pooled from three separate experiments with each datapoint representing an individual biological replicate. Data were analyzed with Prism for a two tailed unpaired T-test analysis. The black bars represent the mean while the blue or red bars indicate ± SEM.

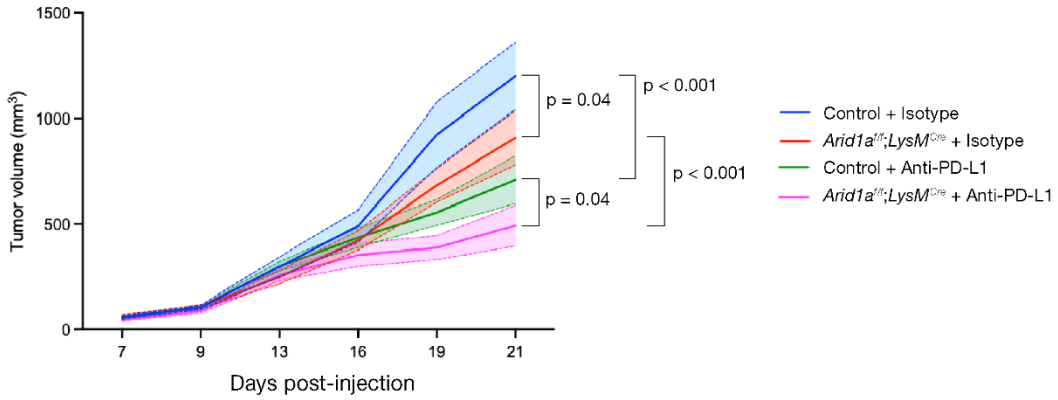

Figure 2. *Arid1a* loss in tumor associated macrophages (TAMs) enhance reduction of tumors treated with anti-PD-L1 therapy.

Control and Arid1a-deficient macrophage (*Arid1a*KO) mice were subcutaneously injected with MC38 tumor cells. Mice with similarly sized tumors were grouped together (day 12) and dosed with either isotype control or anti-PD-L1treatment at 200 µg i.p on days 13, 16, and 19. Average tumor volume (mm^3) of control + isotype (blue), control + anti-PD-L1 (red), *Arid1a*KO + isotype (green), and *Arid1a*KO + anti-PDL1 (pink) in MC38-tumor bearing mice. n=12 isotype-treated control, n=11 isotype treated *Arid1a*$^{f/f}$*; LysM*^{Cre}, n=20 anti-PD-L1 treated control, n=20 anti-PD-L1 treated *Arid1a*$^{f/f}$*; LysM*^{Cre}. Tumor growth curves are displayed as mean (solid line) ± SEM (shaded areas) and were analyzed with Prism using mixed-effects analysis followed by multiple comparison testing, corrected using Turkey's post-hoc test. P-value indicates result from multiple-comparison test on day 21.

1.4 Hypotheses and Aims

Based on these preliminary data, I developed the following hypotheses to test in my master's project:

1. Loss of *Arid1a* in macrophages results in upregulation of PD-L1 and CD86
2. Regulation of PD-L1 and CD86 expression occurs cell intrinsically
3. *Arid1a*-deficient macrophages display enhanced phagocytic ability and are the primary immune cells mediating tumor cell lysis

The primary objective of this thesis was to successfully recapitulate the *in vivo* effects of *Arid1a* loss in an *in vitro* system using bone marrow derived macrophages (BMDMs) in addition to interrogating the mechanisms behind it. Furthermore, I aimed to begin investigation into the cellular mechanism underlying the anti-tumor activity of *Arid1a*-deficient TAMs by testing the hypothesis that *Arid1a*-deficient TAMs might have increased phagocytosis.

Specifically, I aimed to:

1. Utilize bone marrow derived macrophages (BMDMs) to investigate whether PD-L1 and CD86 upregulation occurs in *Arid1a*-deficient macrophages *in vitro*.
2. Utilizing the same BMDM model, determine in what manner PD-L1 and CD86 are upregulated and by which signaling pathways.
3. Using an *in vivo* model, determine if *Arid1a*-deficient TAMs display altered phagocytosis function.

RESULTS

1. Arid1a loss upregulates PD-L1 and CD86 expression, in vitro.

We opted to use an *in vitro* system of bone marrow derived macrophages (BMDMs) to recapitulate the observed preliminary findings. We harvested bone marrow from the femurs of control and *Arid1a*KO mice. If mice were under the UBC^{Cre} promoter, tamoxifen was added on day 4 to induce deletion of *Arid1a* in macrophages. Because we previously found upregulation of interferon stimulated genes, we opted to stimulate cells on day 7 with IFNγ (Figure 1). BMDMs were harvested on day 8 and subsequently analyzed via flow cytometry (Figure 3A). To verify that *Arid1a* was efficiently deleted in our BMDMs we performed flow cytometry after staining intracellularly with an ARID1A antibody. Compared to the control BMDMs, *Arid1a*KO BMDMs did not fluoresce, indicating an absence ARID1A, effectively demonstrating that *Arid1a* was efficiently deleted in the bone marrow derived macrophages under the *Cx3cr1-Cre* promoter (Figure 3B).

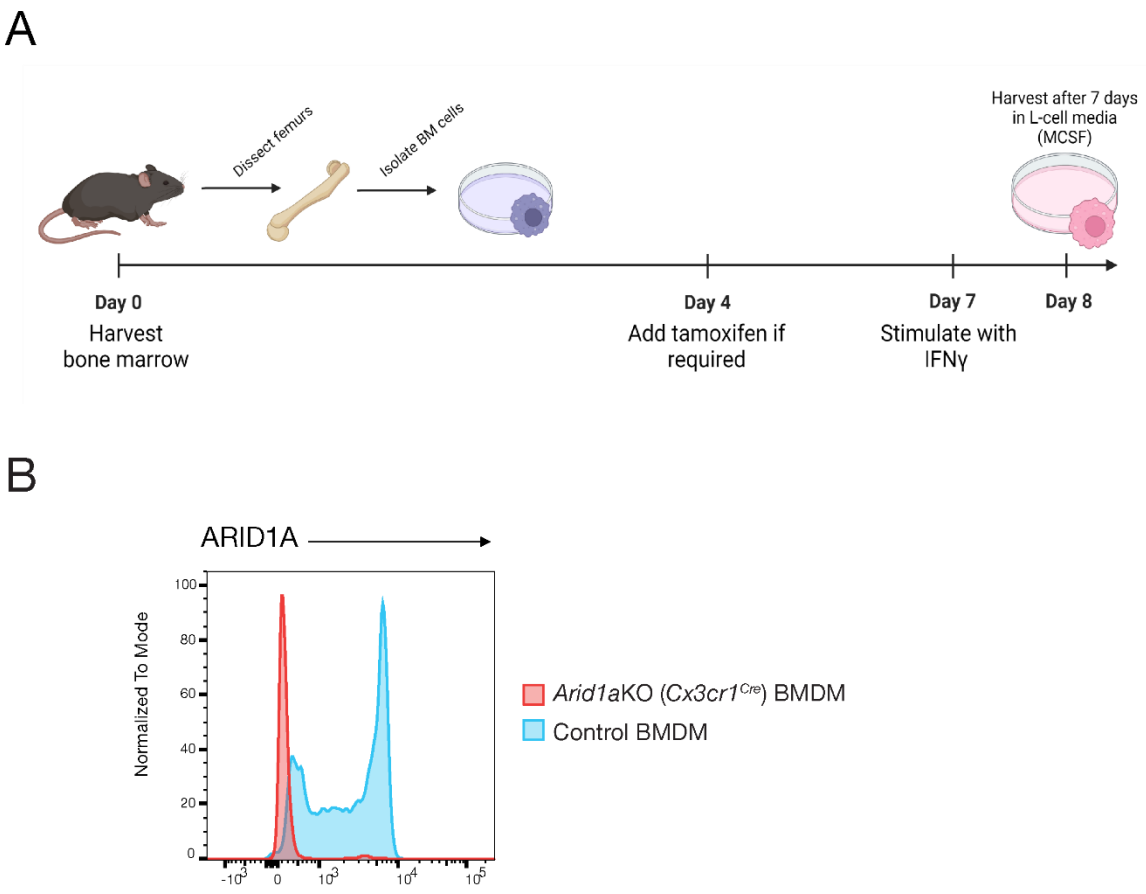

Figure 3. ARID1A is efficiently deleted in bone marrow derived macrophages (BMDMs).

Bone marrow isolated from control and *Arid1a*-deficient macrophage (*Arid1a*KO) mice were harvested and cultured. **A)** Experimental schematic depicting the culture of BMDMs. **B)** Histogram depicting binding of ARID1A. Schematic figure was created with Biorender.com

After verifying deletion of *Arid1a* in BMDMs under the *Cx3cr1-Cre* promoter, we sought to recapitulate the upregulation of PD-L1 and CD86 expression as observed on TAMs. Under the *Cx3cr1-Cre* promoter, the *Arid1a* gene deletes early in monocyte development. The representative histograms visually depict a stepwise increase in PD-L1 expression between unstimulated control and *Arid1a*KO BMDMs. This stepwise increase is also exhibited once more between *Arid1a*KO BMDMs and IFNγ-treated

BMDMs and repeats again between the IFNγ-treated *Arid1a*KO macrophages. A stepwise increase in CD86 expression is also present, albeit not as pronounced or prominent visually compared to PD-L1 expression (Figure 4A). Quantitatively, unstimulated *Arid1a*KO BMDMs expressed approximately 20% more PD-L1 compared to *Arid1a*-intact mice. *Arid1a*KO BMDMs treated with IFNγ for 24h expressed approximately 40% more PD-L1 compared to *Arid1a*-intact mice (Figure 4B). Similarly, unstimulated *Arid1a*KO BMDMs expressed 20% more CD86 compared to control mice. *Arid1a*KO BMDMs stimulated with IFNγ also exhibited approximately a 35% increase compared to the control (Figure 4C). In conclusion, both PD-L1 and CD86 are upregulated upon *Arid1a* loss driven by Cre-recombinase expression under the *Cx3cr1* promoter.

Figure 4. *Arid1a*-deficient bone marrow derived macrophages (BMDMs) upregulate PD-L1 and CD86.

Bone marrow derived macrophages (BMDMs) were harvested from control and genetic knockout models of *Arid1a* deficiency (*Arid1a*KO). PD-L1 and CD86 cell-surface expression levels were quantified using the median fluorescent intensity (MFI). **A)** Representative histogram depicting expression of PD-L1 and CD86 in the indicated groups. **B)** Quantification of normalized MFI of PD-L1 on unstimulated (n=6 for both control and *Arid1a*KO) and IFNγ-treated at 0.2 ng/mL (n=3 for both control and *Arid1a*KO) BMDMs. **C)** Quantification of normalized MFI of CD86 on unstimulated (n=6 for both control and *Arid1a*KO) and IFNγ-treated at 0.2 ng/mL (n=3 for both control and *Arid1a*KO) BMDMs. Data here is pooled from three separate experiments with each datapoint representing an individual biological replicate. All data were normalized to the average of controls within each experiment. Data were analyzed with Prism for a two tailed unpaired T-test analysis. The black bars represent the mean while the blue or red bars indicate ± SEM.

A

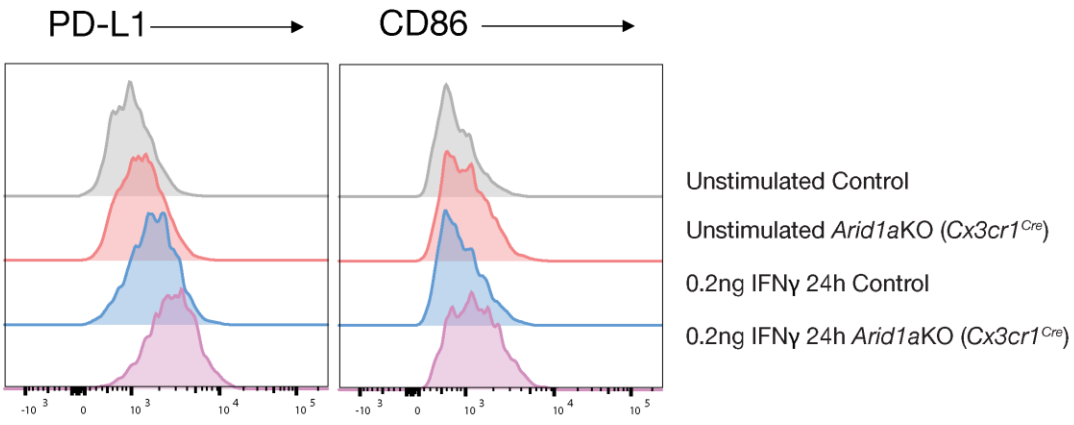
PD-L1
CD86
Unstimulated Control
Unstimulated Arid1aKO (Cx3cr1Cre)
0.2ng IFNγ 24h Control
0.2ng IFNγ 24h Arid1aKO (Cx3cr1Cre)

B

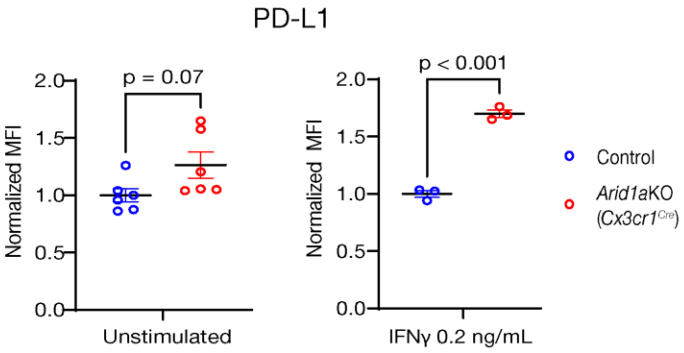
PD-L1
p = 0.07
p < 0.001
Normalized MFI
Unstimulated
IFNγ 0.2 ng/mL
Control
Arid1aKO
(Cx3cr1Cre)

C

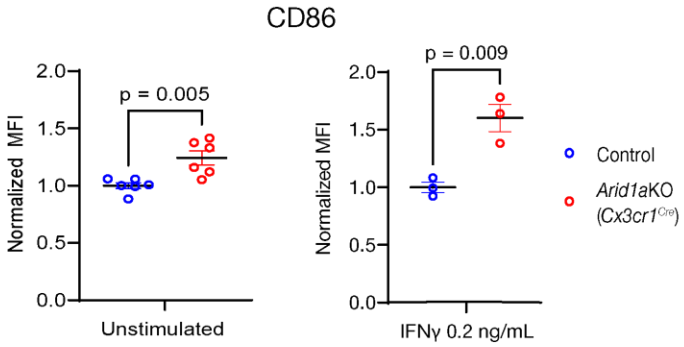
CD86
p = 0.005
p = 0.009
Normalized MFI
Unstimulated
IFNγ 0.2 ng/mL
Control
Arid1aKO
(Cx3cr1Cre)

Previously, we determined that *Arid1a* loss upregulates expression of PD-L1 and CD86 when deleted by Cre-recombinase expressed under the *Cx3cr1* promoter. Next, we hypothesized that acute loss of *Arid1a* or inhibition of ARID1A would also result in upregulation of PD-L1 and CD86. We utilized two different models for acute targeting of ARID1A. The first model utilized a tamoxifen inducible Cre-lox system under the *UBC* promoter. Under this promoter, the *Arid1a* gene would delete during macrophage differentiation. We followed the same protocol previously described and depicted in Figure 3A and verified deletion of *Arid1a* (Figure S2). However, to induce deletion of *Arid1a* in BMDMs, tamoxifen was added on day 4. As predicted, acute loss of *Arid1a* upregulated expression of PD-L1 and CD86. The *Arid1a*KO BMDMs exhibited between a 45% increase in PD-L1 compared to the control. Similarly, the *Arid1a*KO BMDMs exhibited approximately a 35% increase in CD86 compared to the control (Figure 5A).

The second model for acute loss utilized 10 μM of BD98, an ARID1A specific BAF inhibitor, for 24 hours. The control, BMDMs treated with DMSO, simulated *Arid1a*-intact macrophages while BMDMs treated with BD98 simulated *Arid1a*KO macrophages. Like the first model, inhibition of ARID1A resulted in an upregulation of PD-L1 and CD86 expression. BMDMs treated with BD98 exhibited approximately a 22% increase in PD-L1 compared to those treated with DMSO. Similarly, BMDMs treated with BD98 also exhibited approximately a 23% increase in CD86 compared to those treated with DMSO (Figure 5B). These models together demonstrate that acute loss or inhibition of ARID1A also upregulates expression of PD-L1 and CD86.

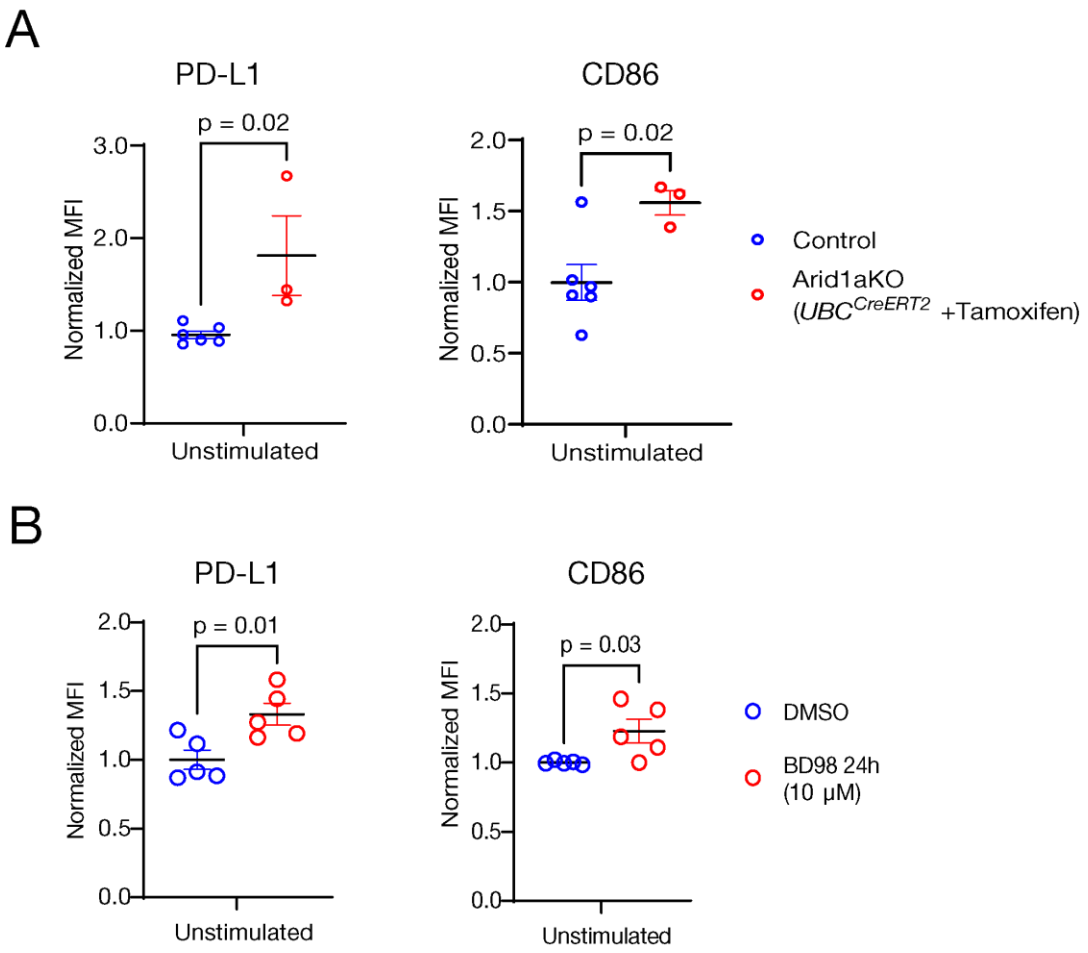

Figure 5. Acute loss of ARID1a *in vitro* phenocopies upregulation of PD-L1 and CD86 in bone marrow derived macrophages (BMDMs).

Bone marrow derived macrophages (BMDMs) were harvested from control and genetic knockout models of *Arid1a* deficiency (*Arid1a*KO) or subjected to BD98, a BAF inhibitor that specifically targets ARID1A. PD-L1 and CD86 cell-surface expression levels were quantified using the median fluorescent intensity (MFI). **A)** Quantification of normalized MFI of PD-L1 and CD86 between control (n=6) and *Arid1a*KO BMDMs (n=3) when unstimulated and IFNγ-treated at 0.2 ng/mL. Data here is pooled from two separate experiments with each datapoint representing an individual biological replicate. **B)** Quantification of normalized MFI of PD-L1 and CD86 between control and BD98-treated BMDMs when unstimulated. Data here is pooled from two separate experiments with three of the datapoints of each condition representing biological replicates (from *Arid1a*$^{f/f}$*Cx3cr1*$^{+/+}$ control genotype mice) and two datapoints from each condition representing a separate cell-culture from one wild-type mouse. All data were normalized to the average of controls within each experiment.

2. *PD-L1 and CD86 expression is JAK1/2 and Type I IFN signaling independent, in vitro.*

As previously observed, both PD-L1 and CD86 genes were found to be upregulated upon interferon stimulation. Previous studies have also indicated expression of both genes can occur through several other cytokines like IL-6, IFNγ, IFNβ, and others. These cytokines operate through a variety of signaling pathways. A primary component in many of these signal transduction pathways is the tyrosine kinase protein, JAK1/2 [26]. To account for the various pathways by which cytokine signaling occurs, we opted to utilize JAKi, and JAK1/2 inhibitor. Since we previously observed the upregulation of interferon stimulated genes (Figure 1) and additionally detected the presence of other type I IFNs in the tumor interstitial fluid (Figure S1), we also opted to block type I IFN signaling with anti-IFNAR. We hypothesized that PD-L1 and CD86 upregulation would be dependent on type I IFN and/or JAK1/2 signaling. We utilized the same genetic knockout model of Arid1a previously described in Figure 3, but with differing treatments. BMDMs treated with DMSO functioned as a control for the cells treated with JAKi, while BMDMs treated with the isotype antibody acted as a control for cells treated with anti-IFNAR.

As previously observed, *Arid1a*KO cells displayed increased PD-L1 expression compared to control cells. Treatment with DMSO or JAKi does not appear to alter expression of PD-L1 in *Arid1a*KO cells (Figure 6A). In both cases, the *Arid1a*KO cells appear to exhibit relatively similar levels of PD-L1 expression, signifying that PD-L1 upregulation upon ARID1A loss is not dependent on JAK1/2 signaling. Similarly, *Arid1a*KO cells appear to express equivalent levels of PD-L1 expression regardless of

isotype or anti-IFNAR treatment. Thus, PD-L1 expression is also not dependent on type I IFN signaling.

In agreement with our previous results, *Arid1a*KO cells displayed increased CD86 expression compared to control cells. Like PD-L1 expression, treatment with DMSO or JAKi does not appear to alter expression of CD86 in *Arid1a*KO cells (Figure 6B). We observe in both conditions CD86 expression is equivalent, further indicating this upregulation is JAK1/2 independent. We also observe that *Arid1a*KO BMDMs express nearly identical levels of CD86 when isotype treated or anti-IFNAR treated. These results also indicate that CD86 expression is independent of type I IFN signaling. To summarize, the results demonstrate that upregulation of PD-L1 and CD86 caused by ARID1A deficiency is not dependent on JAK1/2 and type I IFN signaling.

Figure 6. PD-L1/CD86 upregulation in *Arid1a*KO bone marrow derived macrophages (BMDMs) is not dependent on JAK 1/2 or Type I IFN signaling.

Bone marrow derived macrophages (BMDMs) were harvested from control and genetic knockout models of *Arid1a* deficiency (*Arid1a*KO). PD-L1 and CD86 cell-surface expression levels were quantified using the median fluorescent intensity (MFI). **A)** Quantification of normalized MFI of PD-L1 between control (n=7) and *Arid1a*KO (n=7) BMDMs treated with DMSO, JAKi (JAK1/2 inhibitor), an isotype antibody, and anti-IFNAR. **B)** Quantification of normalized MFI of CD86 between control (n=7) and *Arid1a*KO (n=7) BMDMs incubated with DMSO, JAKi (JAK1/2 inhibitor), an isotype antibody, and anti-IFNAR. Each datapoint represents an individual biological replicate. All data were normalized to the average of controls within each experiment. Data were analyzed with Prism for a two tailed unpaired T-test analysis. The black bars represent the mean while the blue or red bars indicate ± SEM

A

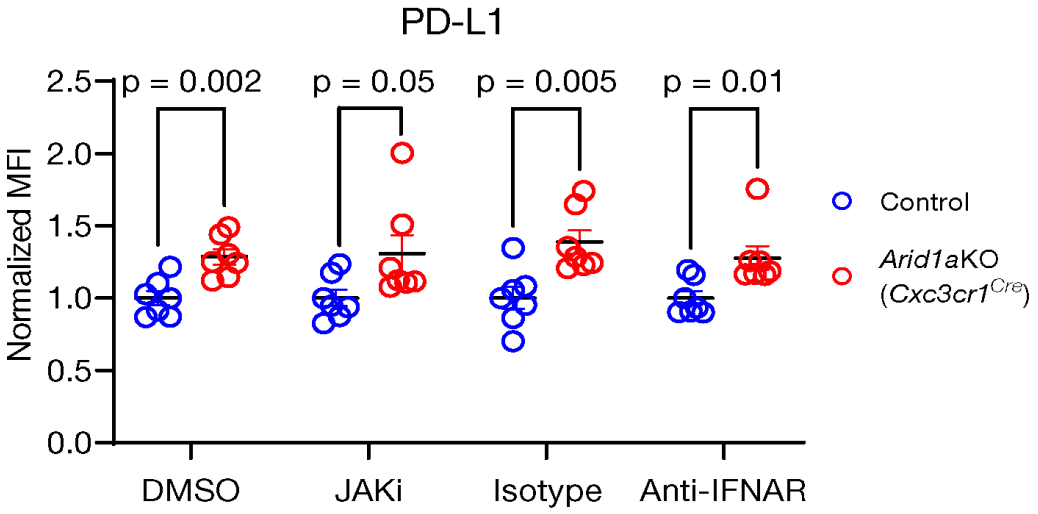
PD-L1
p = 0.002
p = 0.05
p = 0.005
p = 0.01
Normalized MFI
2.5
2.0
1.5
1.0
0.5
0.0
DMSO
JAKi
Isotype
Anti-IFNAR
Control
Arid1aKO
(Cxc3cr1Cre)

B

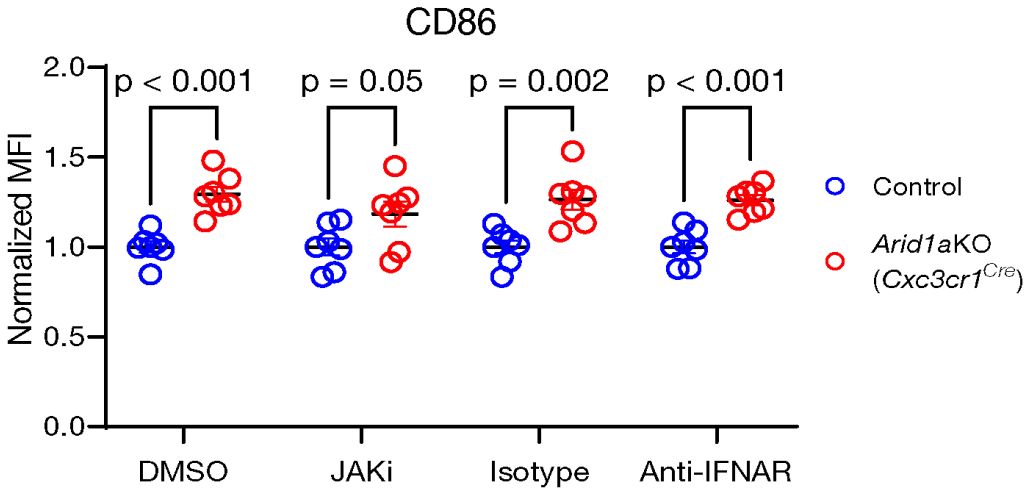
CD86
p < 0.001
p = 0.05
p = 0.002
p < 0.001
Normalized MFI
2.0
1.5
1.0
0.5
0.0
DMSO
JAKi
Isotype
Anti-IFNAR
Control
Arid1aKO
(Cxc3cr1Cre)

3. PD-L1 and CD86 expressions operate via a cell intrinsic manner, in vitro.

Although our previous data indicated that interferon signaling does not regulate PD-L1 or CD86 expression in *Arid1a*KO BMDMs, regulation of these may still be mediated through additional intrinsic of extrinsic mechanisms. We sought to determine if PD-L1 and CD86 were upregulated in a cell-intrinsic or cell-extrinsic mechanism in *Arid1a*KO BMDMs. We utilized the same genetic knockout model of *Arid1a*, and stimulations previously described in Figure 3. The experimental schematic of the co-culture BMDM system used depicts possible results obtained. We utilized CD45.1+ and CD45.2+ to distinguish between test and co-cultured cells. The control co-culture consisted of wild-type CD45.2+ cells alongside wild-type CD45.1+ cells. The test co-culture consisted of *Arid1a*KO CD45.2+ cells alongside wild-type CD45.1+ cells. If upregulation of PD-L1 and CD86 occurred via some cell intrinsic mechanism, we hypothesized that within the test (knockout) co-culture only *Arid1a*KO CD45.2+ cells would exhibit an increase in PD-L1 and/or CD86 compared to the wild-type CD45.1+ cells. If upregulation of PD-L1 and CD86 occurred via some cell extrinsic mechanism, we hypothesized that within the test co-culture both *Arid1a*KO CD45.2+ cells and wild-type CD45.1+ cells would exhibit an increase in PD-L1 and/or CD86 due to paracrine signaling factors (Figure 7A).

As expected, the control co-culture experienced no change in PD-L1 expression between control-genotype CD45.2+ and wild-type CD45.1+ cells. As previously observed, *Arid1a*KO CD45.2+ cells displayed increased PD-L1 expression compared to control-genotype CD45.2+ cells. In the knockout co-culture, both the unstimulated and IFNγ-treated *Arid1a*KO CD45.2+ cells exhibited approximately a 25% increase in PD-L1 expression compared to their wild-type co-cultured CD45.1+ cells, indicating

upregulation of PD-L1 occurs only in *Arid1a*KO cells, and not in neighboring cells hence upregulation occurs via a cell-intrinsic mechanism (Figure 7B).

Likewise, the control co-culture experienced no change in CD86 expression between control-genotype CD45.2+ and wild-type CD45.1+ cells. Again, in concordance with previous results, the *Arid1a*KO CD45.2+ cells exhibited increased CD86 expression compared to control-genotype cells. In the knockout co-culture, the unstimulated *Arid1a*KO CD45.2+ cells also exhibited approximately a 25% increase in CD86 expression compared to their wild-type co-cultured CD45.1+ cells. The IFNγ-treated *Arid1a*KO CD45.2+ cells exhibited approximately a 30% increase in comparison to their wild-type co-cultured CD45.1+ cells (Figure 7C). Based on our results, upregulation of both PD-L1 and CD86 occurs via a cell intrinsic mechanism.

Figure 7. PD-L1 and CD86 are upregulated via a cell intrinsic manner in unstimulated *Arid1a*KO bone marrow derived macrophages (BMDMs).

Control and Arid1aKO CD45.2+ bone marrow derived macrophages (BMDMs) were co-cultured with CD45.1+ BMDMs. PD-L1 and CD86 expressions were quantified using the median fluorescent intensity (MFI). **A)** Experimental schematic depicting co-culture set-up and possible results. **B)** PD-L1 expression between control (n=3) and *Arid1a*KO (n=3) co-cultures on unstimulated and IFNγ-treated BMDMs. **C)** CD86 expression between control (n=3) and *Arid1a*KO (n=3) co-cultures on unstimulated and IFNγ-treated BMDMs. Data were analyzed with one-way ANOVA followed by Fisher's LSD test post-hoc. Lines connecting datapoints in B-C indicate cells that were cultured in the same well. Schematic figure was created with Biorender.com.

A

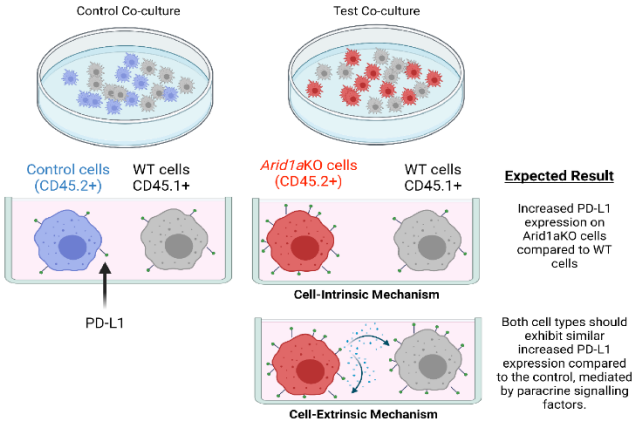
Control Co-culture
Test Co-culture
Control cells (CD45.2+)
WT cells CD45.1+
Arid1aKO cells (CD45.2+)
WT cells CD45.1+
PD-L1
Cell-Intrinsic Mechanism
Cell-Extrinsic Mechanism
Expected Result
Increased PD-L1 expression on Arid1aKO cells compared to WT cells
Both cell types should exhibit similar increased PD-L1 expression compared to the control, mediated by paracrine signalling factors.

B

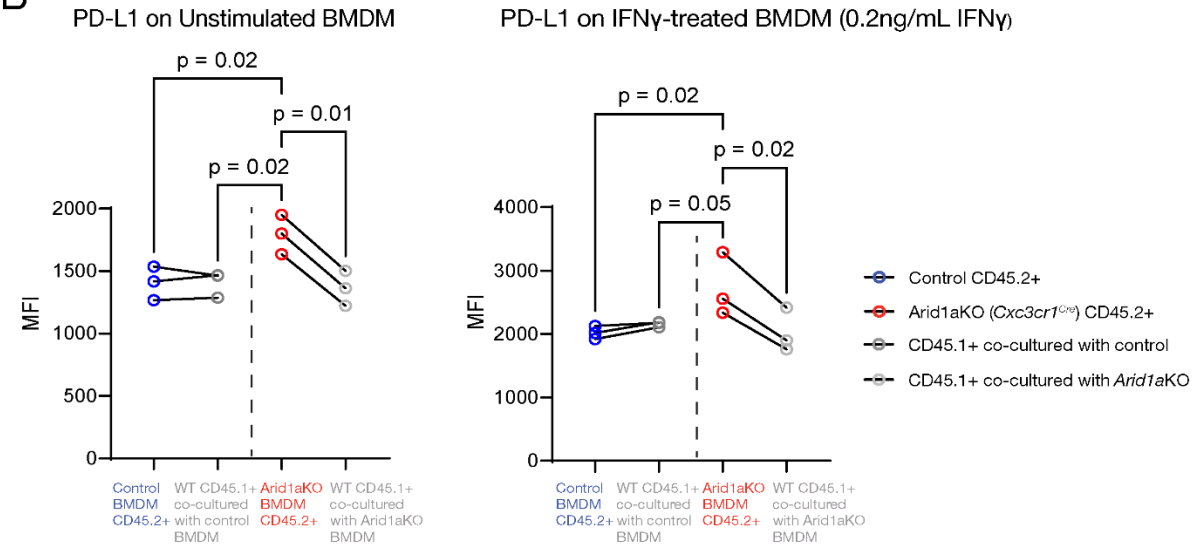
PD-L1 on Unstimulated BMDM
PD-L1 on IFNγ-treated BMDM (0.2ng/mL IFNγ)
p = 0.02
p = 0.01
p = 0.02
p = 0.02
p = 0.02
p = 0.05
MFI
2000
1500
1000
500
0
4000
3000
2000
1000
0
Control BMDM CD45.2+
WT CD45.1+ co-cultured with control BMDM
Arid1aKO BMDM CD45.2+
WT CD45.1+ co-cultured with Arid1aKO BMDM
Control CD45.2+
Arid1aKO (Cxc3cr1Cre) CD45.2+
CD45.1+ co-cultured with control
CD45.1+ co-cultured with Arid1aKO

C

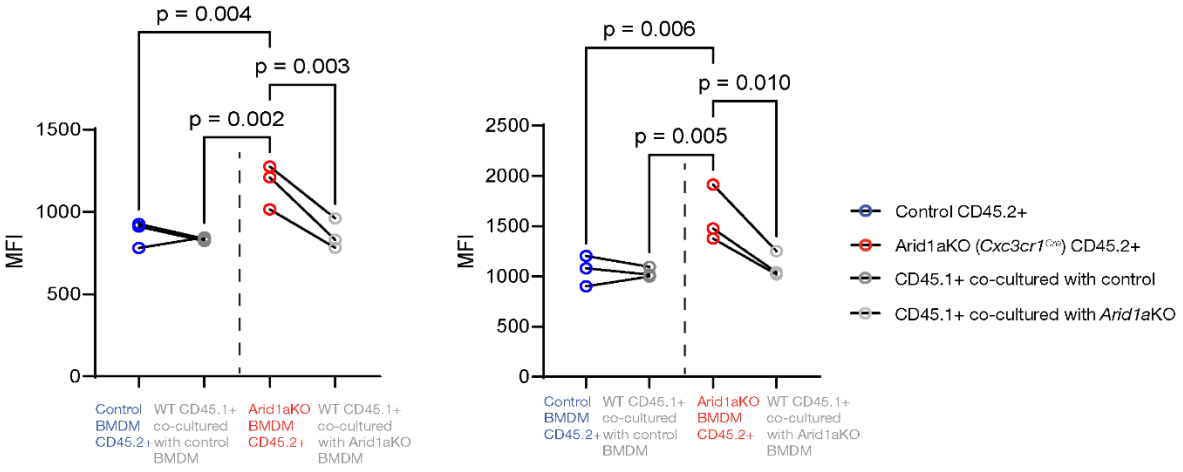
CD86 on Unstimulated BMDM
CD86 on IFNγ-treated BMDM (0.2 ng/mL IFNγ)
p = 0.004
p = 0.003
p = 0.002
p = 0.006
p = 0.010
p = 0.005
MFI
1500
1000
500
0
2500
2000
1500
1000
500
0
Control BMDM CD45.2+
WT CD45.1+ co-cultured with control BMDM
Arid1aKO BMDM CD45.2+
WT CD45.1+ co-cultured with Arid1aKO BMDM
Control CD45.2+
Arid1aKO (Cxc3cr1Cre) CD45.2+
CD45.1+ co-cultured with control
CD45.1+ co-cultured with Arid1aKO

4. *Arid1a-deficient TAMs do not display enhanced phagocytic capabilities, in vivo.*

Prior experiments demonstrated that the most robust reduction in tumor growth occurred in the *Arid1a*KO groups treated with anti-PD-L1 therapy (Figure 2). We sought to assess if the observed tumor reduction was a result of enhanced phagocytic capabilities in TAMs. We hypothesized that *Arid1a*KO TAMs would display increased phagocytic abilities compared to TAMs with *Arid1a*-intact. To assess phagocytosis in TAMs, we developed an *in vivo* system. On day 1 we subcutaneously injected mice with MC38-tdTomato cells and recorded tumor growth on days 7, 9, and 12. After grouping similarly sized tumors together on day 12, we injected the mice with either isotype control or anti-PD-L1 treatment on days 13, 16, and 19. On day 21 tumor cells were harvested and subsequently analyzed via flow cytometry (Figure 8A).

In concordance with our previous results, anti-PD-L1-treated controls displayed almost a 30% reduction in average tumor burden compared to isotype-treated controls. Likewise, the anti-PD-L1-treated *Arid1a*-deficient mice also displayed approximately a 40% reduction in average tumor volume compared to isotype-treated *Arid1a*-deficient mice. Again, when comparing between the isotype-treated control and isotype-treated *Arid1a*KO mice or between anti-PD-L1-treated control and *Arid1a*KO mice, there was a pronounced reduction in average tumor size. Between the isotype-treated control and knockout mice, we observed nearly a 36% decrease in average tumor volume. Between anti-PD-L1-treated control and *Arid1a*KO mice, a similar effect is observed, there the knockout mice have a 43% average decrease in tumor volume (Figure 8B). Based on these results, the MC38-tdTomato cell line exhibits a similar average tumor growth curve

as our previous MC38 cell line, thus indicating that the addition of tdTomato to MC38 cells does not significantly alter tumor growth.

To identify phagocytosing TAMs, we gated only on TAMs that were positive for tomato expression. We suspected there may be difficulties distinguishing between tomato positive and non-tomato positive TAMs and included MC38 as a negative control. We gated our cells based on the negative control to ensure we only captured TAMs that were truly phagocytosing, as the negative control would contain no tomato positive TAMs. The representative gates do not appear to demonstrate any differences in phagocytosing TAMs between treatment groups (Figure 8C). Quantitatively, our results reflect this observation. We observed approximately a 12% decrease in percentage of anti-PD-L1 treated control TAMs compared to isotype-treated control TAMs. Similarly, percentage of *Arid1a*KO TAMs treated with anti-PD-L1 decreased by approximately 6% when compared to isotype-treated *Arid1a*KO TAMs. In contrast, the percentage of isotype-treated *Arid1a*KO TAMs exhibited approximately a 4% increase compared to isotype- treated control TAMs. Likewise, the percentage of anti-PD-L1 treated *Arid1a*KO TAMs exhibited approximately a 10% increase compared to anti-PD-L1 treated control TAMs (Figure 8D). These results further suggest that both *Arid1a* and treatment group have minimal effects on the percentage of TAMs phagocytosing.

To determine the amount TAMs phagocytosed tomato+ tumor cells, we quantified the median fluorescent intensity (MFI) of tomato+ TAMs. We observed approximately less than a 1% increase in tomato expression in anti-PD-L1 treated control TAMs compared to isotype-treated control TAMs. Similarly, expression of tomato in *Arid1a*KO TAMs treated with anti-PD-L1 increased slightly by approximately 4% when compared

to isotype-treated *Arid1a*KO TAMs. Similarly, there was a 4% increase in tomato expression in isotype-treated *Arid1a*KO TAMs compared to isotype-treated control TAMs. Anti-PD-L1 treated *Arid1a*KO TAMs exhibited approximately an 8% increase in tomato expression compared to anti-PD-L1 treated control TAMs. However, these increases are not only minimal at best, but also insignificant (Figure 8E). Taken together, these results do not agree with our hypothesis that *Arid1a*KO TAMs would exhibit enhanced phagocytic ability. Rather our results indicate that loss of *Arid1a* driven by Cre-recombinase expression under the *LysM* promoter has no effect on the phagocytic abilities of TAMs.

Figure 8. Testing *in vivo* phagocytosis capacity of TAMs.

Control and *Arid1a*-deficient macrophage (*Arid1a*KO) mice were subcutaneously injected with MC38-tdTomato tumor cells. Mice with similarly sized tumors were grouped together (day 12) and dosed with either isotype control or anti-PD-L1treatment at 200 μg i.p on days 13, 16, and 19. Tomato+ cell-surface expression levels were quantified using the median fluorescent intensity (MFI). **A)** Experimental schematic depicting an *in vivo* functional assay for phagocytosis. **B)** Average tumor volume (mm^3) of control + isotype (blue), control + anti-PD-L1 (red), *Arid1a*KO + isotype (green), and *Arid1a*KO + anti-PDL1 (pink) MC38-tumor bearing mice. n=3 isotype-treated control, n=5 isotype treated *Arid1a*KO, n=5 anti-PD-L1 treated control, n=6 anti-PD-L1 treated *Arid1a*KO. **C)** Representative gating strategy of TAMs collected from MC38-tdTomato tumors treated with either isotype or anti-PD-L1 grown in control or *Arid1a*KO mice and from untreated MC38 tumors grown in control mice. **D)** Quantified percentage of total Tomato+ TAMs identified from MC38-tdTomato tumors treated with isotype or anti-PD-L1 grown in control or *Arid1a*KO mice based on gating strategy shown in Figure 7C. **E)** Quantification of MFI of Tomato+ TAMs from MC38-tdTomato tumors treated with isotype or anti-PD-L1 grown in control or *Arid1a*KO mice. Data were analyzed with one-way ANOVA followed by Fisher's LSD test post-hoc. The black bars represent the mean while the blue, red, green, or pink bars indicate ± SEM. Schematic figure was created with Biorender.com.

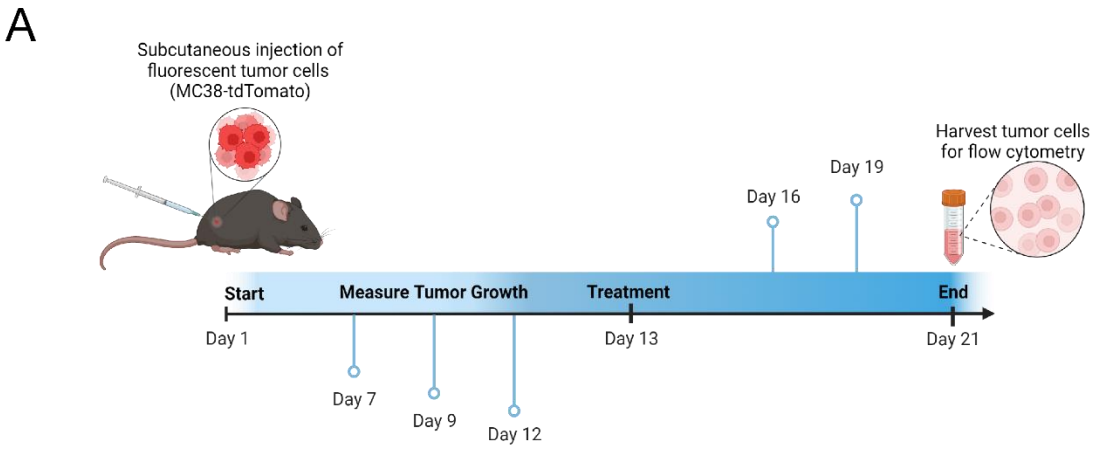
A
Subcutaneous injection of fluorescent tumor cells (MC38-tdTomato)
Harvest tumor cells for flow cytometry
Day 16
Day 19
Start
Measure Tumor Growth
Treatment
End
Day 1
Day 7
Day 9
Day 12
Day 13
Day 21

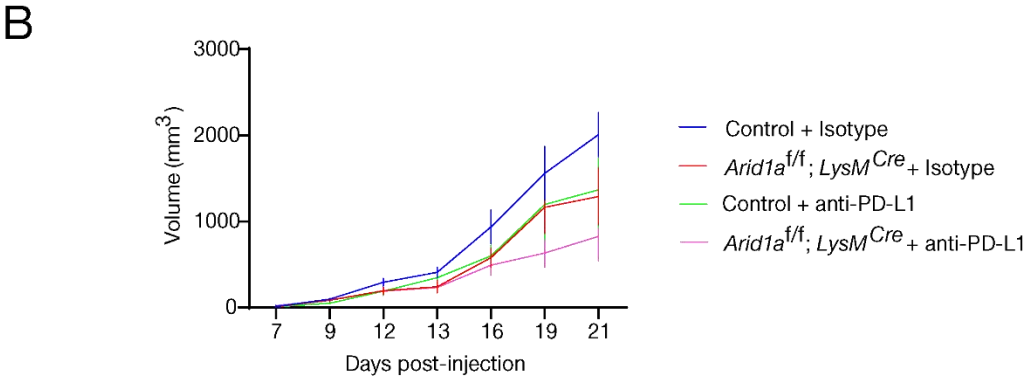
B
3000
2000
1000
0
Volume (mm3)
7
9
12
13
16
19
21
Days post-injection
Control + Isotype
Arid1af/f; LysMCre + Isotype
Control + anti-PD-L1
Arid1af/f; LysMCre + anti-PD-L1

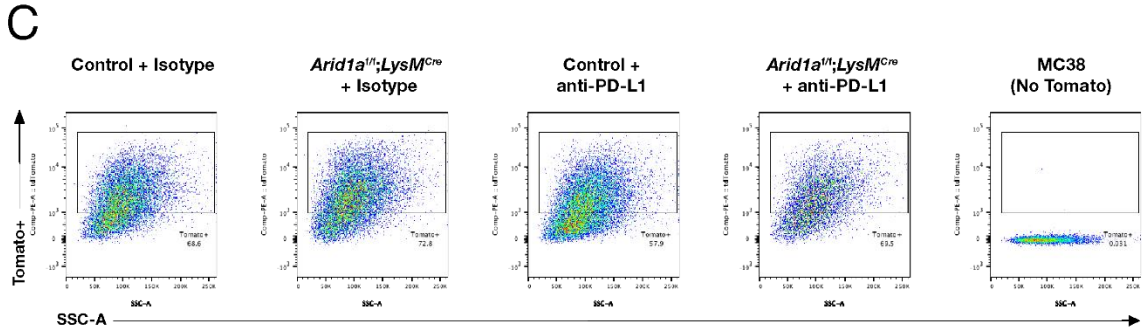
C
Control + Isotype
Arid1af/f;LysMCre + Isotype
Control + anti-PD-L1
Arid1af/f;LysMCre + anti-PD-L1
MC38 (No Tomato)
Tomato+
SSC-A

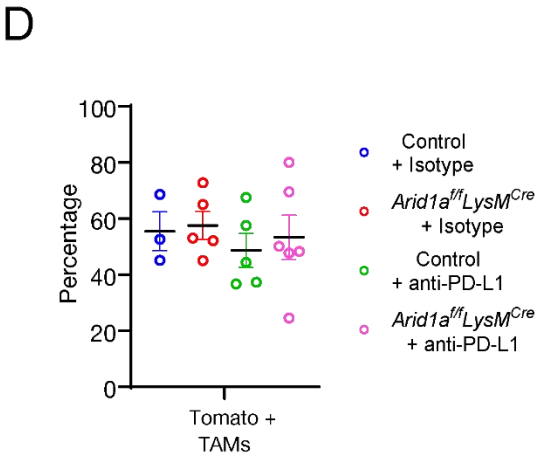
D
100
80
60
40
20
0
Percentage
Tomato + TAMs
Control + Isotype
Arid1af/fLysMCre + Isotype
Control + anti-PD-L1
Arid1af/fLysMCre + anti-PD-L1

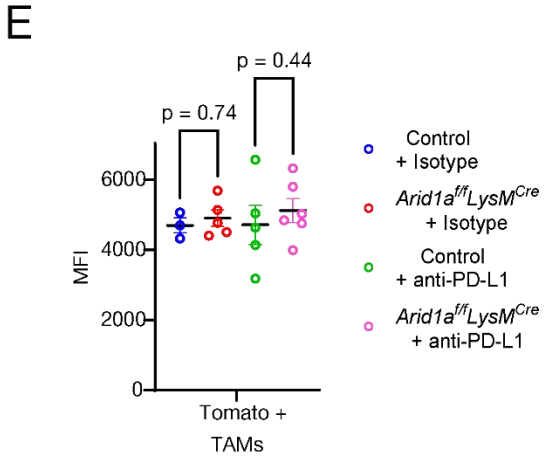
E
p = 0.44
p = 0.74
6000
4000
2000
0
MFI
Tomato + TAMs
Control + Isotype
Arid1af/fLysMCre + Isotype
Control + anti-PD-L1
Arid1af/fLysMCre + anti-PD-L1

DISCUSSION

1. Arid1a epigenetically regulates expression of PD-L1 and CD86 in BMDMs.

A previous study conducted indicates that microglia, the resident macrophages of the central nervous system, isolated *in vivo* display different gene expressions compared to *in vitro* samples [12]. Knowing this we sought to confirm that our *in vitro* model of bone marrow derived macrophages (BMDMs) could recapitulate our preliminary findings. Briefly, our preliminary findings indicated the upregulation of genes in the interferon pathway, specifically *Cd86* and *Cd247* (PD-L1), at both the RNA and protein level (Figure 1). Our results demonstrated that loss of *Arid1a* results in the upregulation of both PD-L1 and CD86. This upregulation was verified under three separate models: the first depicting complete loss of *Arid1a* under the *Cx3cr1* promoter, the second depicting acute loss under the *UBC* promoter, and the third using pharmacological inhibition of ARID1A via BD98 (Figure 4B-C, 5A-B). All three models support our *in vivo* findings, thus validating our strategy to utilize an *in vitro* system of BMDMs to investigate the role of *Arid1a* loss in regulation of CD86 and PD-L1 expression. However, it is possible not all aspects of gene expression seen *in vivo* were recapitulated *in vitro*. Our experiments looked only at the expression of PD-L1 and CD86. To better determine the extent to which this *Arid1a* loss phenotype is replicated *in vitro*, RNAseq should be performed on BMDMs and compared to TAMs isolated *in vivo*.

2. PD-L1 and CD86 expression occurs cell intrinsically

As stated earlier, the presence of cytokines in the tumor microenvironment (TME) can polarize macrophages towards an M1-like or M2-like phenotype. In particular, previous studies have found that expression of proinflammatory cytokines like IL-6, IFNγ, IFNβ, and others can influence the expression of PD-L1 and CD86 [11, 17, 22, 33-34]. To investigate if expression of these cell surface markers occurs via a cell intrinsic or cell extrinsic mechanism we blocked signaling and co-cultured BMDMs. Upon blocking JAK1/2 and Type I IFN signaling, BMDMs exhibited the same upregulation of PD-L1 or CD86 expression in *Arid1a*-deficient (*Arid1a*KO) versus intact cells (Figure 6). This indicated that expression occurred independently of type I interferon signaling, as well as all cytokine signaling pathways that required JAK1/2. To broaden the scope and investigate whether any cell-extrinsic factors were involved we co-cultured BMDMs. Our results indicated that in our test (knockout) co-culture, *Arid1a*KO cells expressed higher PD-L1 and CD86 expression compared to their wild-type co-cultured cells (Figure 7B-C). Both results support our finding that PD-L1 and CD86 are regulated by *Arid1a* via some cell intrinsic mechanism. Taken together with our previous observation regarding ARID1A inhibition, we suspect that ARID1A may function as a repressor. Previous studies have not only demonstrated that ARID1A may have a repressive role but has been found to directly affect transcription of PD-L1 in ovarian cancer cell types [9, 23]. To determine if ARID1A indeed has a repressive role at these gene sites, we can perform ChIP-seq and/or CUT&RUN on macrophages isolated both *in vivo* and *in vitro* to determine ARID1A binding.

3. *The phagocytic activity of Arid1a-deficient TAMs is not the primary immune mechanism mediating tumor reduction*

Both our preliminary data and results show that *Arid1a* loss enhanced anti-PD-L1 therapy (Figure 2, 8B). Prior studies have indicated that the phagocytic activity of TAMs is sufficient in mediating tumor cell destruction in select tumor models [6, 19]. We hypothesized the observed tumor reduction resulted from enhanced phagocytic function in TAMs deficient for *Arid1a*. However, our results indicated that *in vivo* phagocytosis was independent of ARID1A status. We found that TAMs undergoing phagocytosis were present in equivalent proportions in both control and *Arid1a*KO TAMs (Figure 8D). We also observed that our control and *Arid1a*KO TAMs displayed equivalent levels of tomato, which reflects the amount of material taken up from the MC38-tdTomato cells (Figure 8E). Based on our results, it is highly unlikely that TAMs are mediating the tumor reduction observed via enhanced phagocytosis.

We suspect instead that macrophage activation of T cells via enhanced antigen presentation, co-stimulation, and/or cytokine secretion may be the primary immune mechanism mediating tumor cell lysis. It has been well established that PD-L1 and CD86 have roles in T cell activation as co-inhibitory and co-stimulatory molecules respectively [3]. Based on our data, it is plausible that in *Arid1a*-deficient macrophage mice treated with anti-PD-L1 we are simultaneously preventing further T cell inhibition and increasing T cell activation. As we have already shown, loss of *Arid1a* upregulates both PD-L1 and CD86 expression. Increased presence of PD-L1 may enhance anti-PD-L1 therapy by further preventing T cell inhibition, while increased CD86 expression may provide

additional or stronger co-stimulation signals required to activate T cells. To evaluate this further, we could perform an *in vitro* T cell activation assay or deplete T cells *in vivo*.

CONCLUSION

In conclusion, this thesis establishes that our *in vitro* system of bone marrow derived macrophages (BMDMs) successfully recapitulates the observed upregulation of CD86 and PD-L1 in *Arid1a*-deficient macrophages. Our results demonstrate complete and acute loss of *Arid1a* results in the upregulation of PD-L1 and CD86 cell-surface expression. We determined that upregulation was not mediated by either JAK1/2 or Type I IFN signaling and instead operates in a cell intrinsic manner. Furthermore, *Arid1a*-deficient tumor associated macrophages (TAMs) displayed equivalent phagocytic capabilities compared to *Arid1a*-intact TAMs. Further studies are required to determine the extent to which the *Arid1a* loss phenotype can be recapitulated *in vitro* and how ARID1A cell intrinsically upregulates PD-L1 and CD86. However, the work presented here can help further direct and optimize preclinical strategies aimed at reprogramming macrophages as a potential cancer therapeutic.

MATERIALS AND METHODS

1. BMDM Culture

Bone marrow was harvested from the femurs of 8- to 15-wk-old mice and cultured in BMDM media (Table 1) on 10 cm Petri dishes. The cells were incubated in an incubator at 37°C with 5% CO_2. On day 6, cells were lifted using cold phosphate-buffered saline (PBS) and replated onto tissue culture-treated dishes in half D10 media (Table 1) and half BMDM media. On day 7, macrophages were left untreated or stimulated overnight before being harvested for flow cytometry. Where indicated, BMDMs were treated/stimulated with DMSO, IFNγ (0.2 ng/mL), isotype antibody (1 µg/mL), interferon-α/β receptor antibody (IFNAR; 1 µg/mL), or with a JAK1/2 inhibitor (0.5 µM). On day 8 cells were treated with 300 µl of Accutase for 5 min before addition of 700 µL of cold PBS to inactivate the Accutase reaction. BMDM cells were subsequently harvested, washed, and resuspended in cold PBS to achieve a single cell suspension.

Table 1. Media Composition used for *in vitro* models

Media	Content	Manufacturer
BMDM Media	46% RPMI-1640 GlutaMax 20% Fetal bovine serum (FBS) 30% L-Cell Media 1% Hepes 1% Sodium Pyruvate 1% Penicillin/Streptomycin 1% Non-essential amino acids	Fisher Scientific Omega Scientific See Below Hyclone Genesee Scientific Life Technologies Life Technologies
L-Cell Media	L-cells which produce M-CSF were grown in 10% FBS in Dulbecco's modified eagles media (DMEM) with 1% Penicillin/Streptomycin for 7-10 days. The supernatant was harvested, filtered through a 0.22 µm PES membrane filter and subsequently frozen at -80°C [20].	Hyclone Life Technologies
D10 Media	89% DMEM 10% FBS 1% Penicillin/Streptomycin	Hyclone Omega Scientific Life Technologies

2. Cytokine Isolation

On day eight of our BMDM cultures, 200 µL of supernatant was initially collected into a 96-well U-bottom plate. Supernatant was spun at 350xg for 3-5 minutes to remove any additional cellular debris before transferring 180 µL of supernatant into a new 96-well U-bottom plate. The supernatant was snap-frozen on dry ice and stored at -80°C before testing with a Legendplex assay.

3. Legendplex

Supernatant from BMDMs that were previously isolated were used for the Legendplex mouse 13-plex cytokine assay (CAT #740446, Lot #B340961) as per the manufacturer's instruction with the following modification: 15 µL of reagents and supernatant was used.

4. Animals

All mice were housed in a 12-h light, 12-h dark cycle. Mouse experiments were approved by the Institutional Animal Care and Use Committee (IACUC) at the Salk Institute. *Arid1a* mice were generated by the Terry Magnuson laboratory. LoxP sites were inserted flanking exon 5 and 6 [2]. *Arid1a* mice were backcrossed to Jackson Laboratory C57BL6/J strains for at least 10 generations. *LysM-Cre* mice were from Jackson Laboratory (cat. no. 004781). C57BL6/J mice were from Jackson Laboratory (cat. no. 000664).

Table 2. Genotypes of mice used for *in vitro* experiments

Figure 4			
Genotype	**Group**	**Sample Size (n)**	**Stimulation/Treatment**
Arid1a$^{+/+}$; *Cx3cr1*$^{+/Cre}$	Control	3	Unstimulated
Arid1a$^{+/+}$; *Cx3cr1*$^{+/+}$	Control	3	Unstimulated
Arid1a$^{f/f}$; *Cx3cr1*$^{Cre/Cre}$	Knockout	5	Unstimulated
Arid1a$^{f/f}$; *Cx3cr1*$^{+/Cre}$	Knockout	1	Unstimulated
Arid1a$^{+/+}$; *Cx3cr1*$^{+/Cre}$	Control	3	0.2 ng/mL IFNγ
Arid1a$^{f/f}$; *Cx3cr1*$^{+/Cre}$	Knockout	3	0.2 ng/mL IFNγ
Figure 5			
Genotype	**Group**	**Sample Size (n)**	**Stimulation/Treatment**
Arid1a$^{f/f}$*:Tg(UBC-CreERT2* + Ethanol	Control	4	Unstimulated
Arid1a$^{f/+}$*UBC*$^{+/+}$ + Tamoxifen	Control	1	Unstimulated
Arid1a$^{f/f}$ [No Cre transgene] + Tamoxifen	Control	1	Unstimulated
Arid1a$^{f/f}$*:Tg(UBC-CreERT2)* + Tamoxifen	Knockout	3	Unstimulated
Figure 6			
Genotype	**Group**	**Sample Size (n)**	**Stimulation/Treatment**
Arid1a$^{f/f}$*Cx3cr1*$^{+/+}$	Control	3	***DMSO, JAKi, Isotype antibody, & Anti-IFNAR
Arid1a$^{+/+}$*Cx3cr1*$^{+/Cre}$	Control	3	***DMSO, JAKi, Isotype antibody, & Anti-IFNAR
Arid1a$^{+/+}$*Cx3cr1*$^{+/+}$	Control	1	***DMSO, JAKi, Isotype antibody, & Anti-IFNAR
Arid1a$^{f/f}$*Cx3cr1*$^{Cre/Cre}$	Knockout	1	***DMSO, JAKi, Isotype antibody, & Anti-IFNAR
Arid1a$^{f/f}$*Cx3cr1*$^{+/Cre}$	Knockout	6	***DMSO, JAKi, Isotype antibody, & Anti-IFNAR
Figure 7			
Genotype	**Group**	**Sample Size (n)**	**Stimulation/Treatment**
Arid1a$^{+/+}$; *Cx3cr1*$^{Cre/+}$	Control CD45.2	3	***Unstimulated & 0.2 ng/mL IFNγ
Arid1a$^{f/f}$; *Cx3cr1*$^{Cre/+}$	Knockout CD45.2	3	***Unstimulated & 0.2 ng/mL IFNγ
Arid1a$^{+/+}$; *Cx3cr1*$^{Cre/+}$	WT CD45.1	3	***Unstimulated & 0.2 ng/mL IFNγ
Arid1a$^{f/f}$; *Cx3cr1*$^{Cre/+}$	WT CD45.1	3	***Unstimulated & 0.2 ng/mL IFNγ

*** = Treated in separate wells, but isolated from the same mice

Table 3. Genotypes of mice used for *in vivo* experiments

Figure 8			
Genotype	**Group**	**Sample Size (n)**	**Stimulation/Treatment**
Arid1a$^{+/-}$; *LysM*$^{+/Cre}$	Control	1	Isotype
Arid1a$^{+/+}$; *LysM*$^{+/Cre}$	Control	2	Isotype
Arid1a$^{f/f}$; *LysM*$^{+/+}$	Control	1	Anti-PD-L1
Arid1a$^{+/+}$; *LysM*$^{+/Cre}$	Control	4	Anti-PD-L1
Arid1a$^{f/f}$; *LysM*$^{Cre/Cre}$	Knockout	2	Isotype
Arid1a$^{f/f}$; *LysM*$^{+/Cre}$	Knockout	3	Isotype
Arid1a$^{f/f}$; *LysM*$^{Cre/Cre}$	Knockout	1	Anti-PD-L1
Arid1a$^{f/f}$; *LysM*$^{+/Cre}$	Knockout	5	Anti-PD-L1

5. Tumor Models

All animal procedures were performed in accordance with Institutional Animal Care and Use Committee (IACUC) regulations at the Salk Institute. MC38-tdTomato cultured cells were trypsinized and washed twice with cold PBS. 5.0 x 10^5 tumor cells were subcutaneously injected into six- to ten-week-old mice. Mice with similarly sized tumors were grouped together on day 12. Mice were dosed with either isotype control or anti-PD-L1 treatment at 200 ug intraperitoneally (i.p) on days 13, 16, and 19. Tumors cells with a volume of < 90mm^3 by day 13 were excluded. Tumor diameters were measured along 2 axes (x = length, y = width) using calipers on days 7, 9, 12, 13, 16, 19, and 21 post-injections. Tumor volume was calculated using the following formula: volume (mm^3) = [$width^2$ (mm^2) X length (mm)] / 2 [4]. MC38-tdTomato cells were gifted from Kaech lab.

6. TAM Isolation

Tumors were harvested and placed into a 6-well plate with 1 mL of Media 3 (Table 4) on ice. To isolate tumor-infiltrating lymphocytes (TILs), tumors were cut into small fragments and digested with 0.05 µg/µL of Liberase (Roche) and 0.1 mg/mL of DNaseI (Sigma) for 30 min in an incubator at 37°C with 5% CO_2. Tumors were then washed with 5 mL of ice-cold FACS buffer to inactivate Liberase reaction and then subsequently strained through a 70 µm filter. Isolated TILs were incubated for 1-2 with RBC lysis. Addition of 5 mL of FACS buffer was used to halt lysis of red blood cells. Cells were subsequently spun down at 300xg before resuspension with FACS buffer to achieve a single cell suspension.

Table 4. Media Composition used for in vivo models

Media	Composition	Manufacturer
Media 3	RPMI Penicillin/Streptomycin 20 mM Hepes	Fisher Scientific Life Technologies Hyclone
FACS Buffer	PBS 2% FBS 1mM EDTA	Salk Media Core Omega Scientific Sigma-Aldrich

7. Flow Cytometry

Single-cell suspensions (either BMDMs or TILs) were transferred to a U-bottom 96-well plate and first incubated with zombie dye (either NIR or red) in PBS for 15-30 min on ice, covered. After spinning at 350xg for 3-5 min, cells were incubated with FC block in FACS buffer (TILs required an additional 5mM of MgCl2 and maintenance DNAse) for 10-30 min on ice, covered. Single-cell suspensions were stained with relevant antibodies for 30 min – 1hr before being washed twice with FACS buffer. Only TILs isolated from MC38-tdTomato tumor models were required to be analyzed the same day. BMDM cells could be fixed and analyzed the day after. Stained cells were analyzed on a 5-laser FACSymphony A3. Data were analyzed with FlowJo software.

Table 5. List of relevant antibodies used for staining

Cell Marker	Fluorophore	Dilution	Lot #	Cat #	Manufacturer
CD11b	BV480	1/400	2059915	566149	BD Biosciences
CD45	BV711	1/200	B334260	103147	BioLegend
CD45.1	BUV395	1/200	1067115	565212	BD Biosciences
CD45.2	PeCy7	1/200	B355881	109829	BioLegend
CD64	APC	1/200 ***1/100	B357450	139306	BioLegend
CD86	BV605	1/200	13362166	10537	BioLegend
CD86	FITC	1/200	B243722	105006	BioLegend
F480	BV785	1/200 ***1/100	B354876	123141	BioLegend
FC Block	N/A	1/100	P0161070920704	70-0161-U500	Tonbo Biosciences
Ly6C	BV605	1/400	B357153	128036	BioLegend
Ly6G	FITC	1/200	B277117	127606	BioLegend
SigF	BUV395	1/200	216624	740280	BD Biosciences
PD-L1	BUV737	1/200	2238301	741877	BD Biosciences
PD-L1	PE	1/200	B357557	124308	BioLegend
Zombie	NIR	1/2000	B349569	423105	BioLegend
Zombie	Red	1/2000	B258615	423109	BioLegend

*** = Dilution of stains used for *in vivo* cells isolated

8. Statistical Analysis

Excel was used to compile the raw MFI and cytokine data and calculations were performed to normalize the data. GraphPad – PRISM 9 was used to analyze and graph the data. Unpaired t-tests were used to determine statistical significance for *in vitro* experiments. One-way ANOVA analysis was used followed by Fisher's LSD for *in vivo* experiments. Only tumors cells that reached a volume of $\geq 90mm^3$ by day 13 were included.

Supplemental Figures

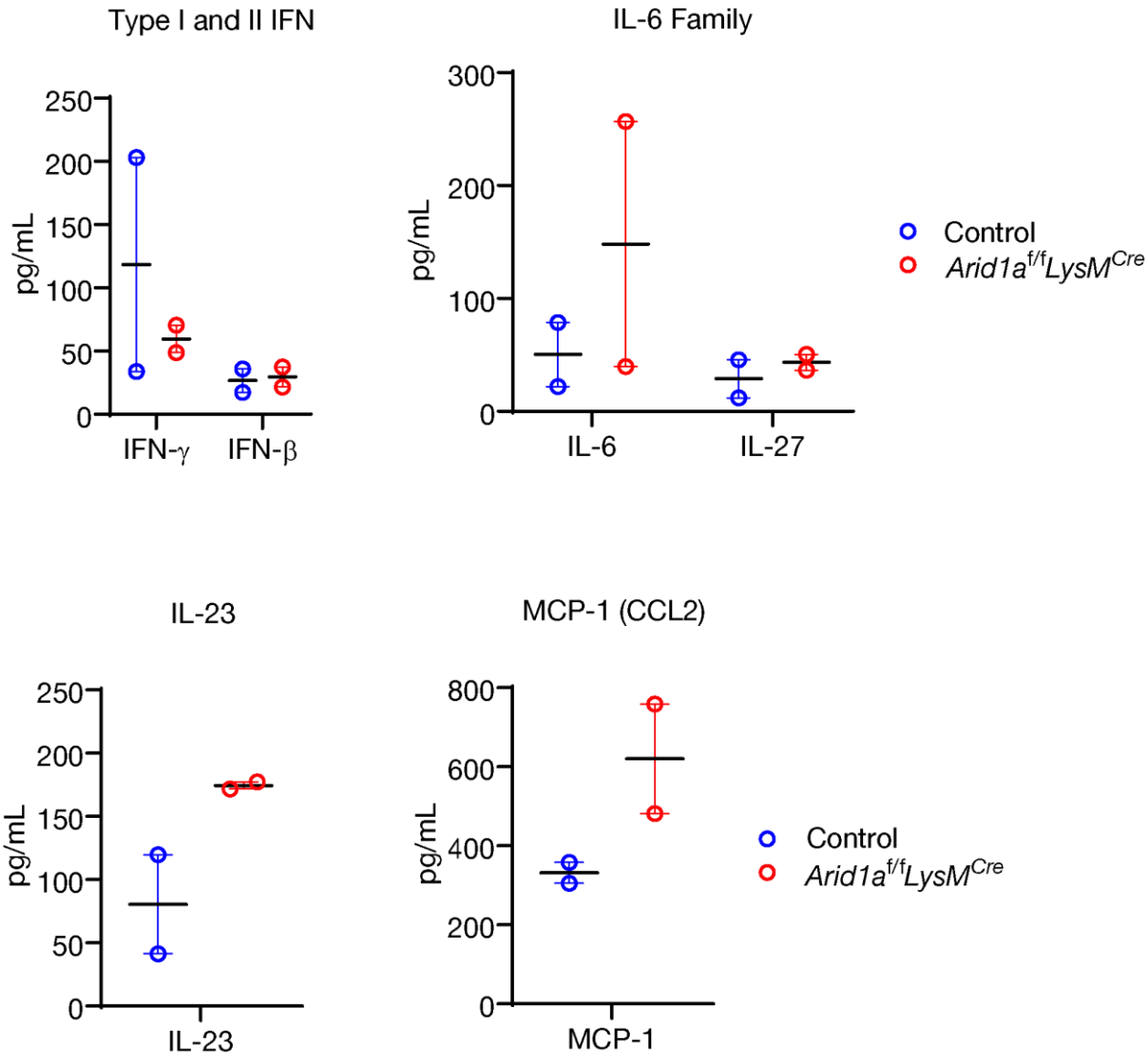

Supplemental Figure 1. Concentration of Inflammatory Cytokines in the tumor interstitial fluid (TIF)

The concentration of inflammatory cytokines was measured with an assay from the interstitial fluid of MC38 tumors. The tumor interstitial fluid (TIF) was isolated from MC38 tumors grown in control and *Arid1a*KO mice. All data were analyzed with Prism. The black bars represent the mean while the blue or red bars indicate ± SEM.

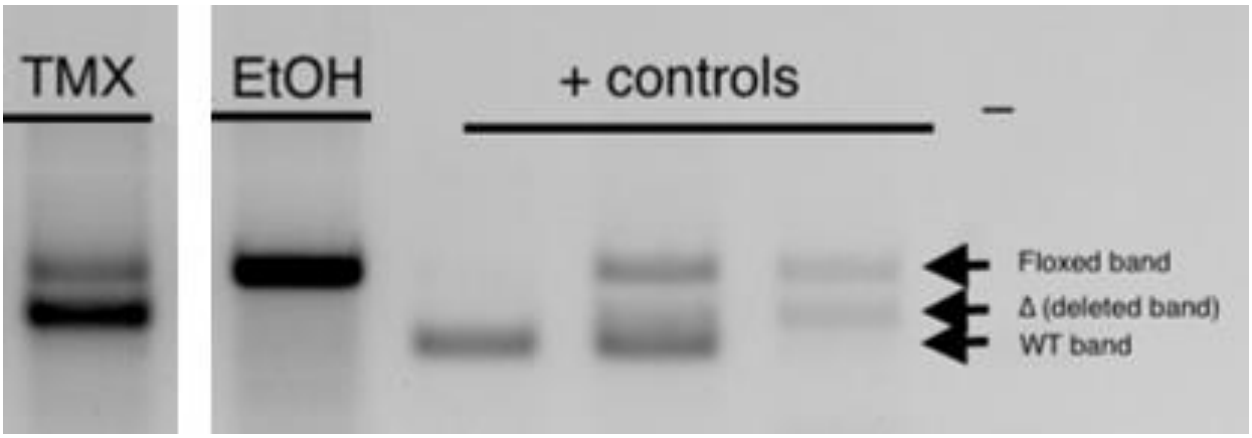

Supplemental Figure 2. Deletion of *Arid1a* under the *UBC* Promoter

Bone marrow derived macrophages (BMDMs) were harvested from *Arid1a*$^{f/f}$*;UBC*$^{+/CreERT2}$ and cultured separately, with one receiving tamoxifen on day 4 to induce deletion of *Arid1a*. Electrophoresis was performed on 2% agarose gel, stained with ethidium bromide, and visualized under U. V. light. The floxed band (top) represents the *Arid1a* gene flanked by lox P sites. The deleted band (middle) indicates deletion of *Arid1a*. The WT band (bottom) represents the *Arid1a* gene with no lox P sites flanked around it.

REFERENCES

1. Cendrowicz, E., Sas, Z., Bremer, E., & Rygiel, T. P. (2021). The Role of Macrophages in Cancer Development and Therapy. *Cancers*, *13*(8), 1946. https://doi.org/10.3390/cancers13081946

2. Chandler, R. L., Damrauer, J. S., Raab, J. R., Schisler, J. C., Wilkerson, M. D., Didion, J. P., Starmer, J., Serber, D., Yee, D., Xiong, J., Darr, D. B., de Villena, F. P.-M., Kim, W. Y., & Magnuson, T. (2015). Coexistent ARID1A–PIK3CA mutations promote ovarian clear-cell tumorigenesis through pro-tumorigenic inflammatory cytokine signalling. *Nature Communications*, *6*(1), 6118. https://doi.org/10.1038/ncomms7118

3. Chen, L., & Flies, D. B. (2013). Molecular mechanisms of T cell co-stimulation and co-inhibition. *Nature Reviews Immunology*, *13*(4), 227–242. https://doi.org/10.1038/nri3405

4. Chen, S., Wang, L., Fan, J., Ye, C., Dominguez, D., Zhang, Y., Curiel, T. J., Fang, D., Kuzel, T. M., & Zhang, B. (2015). Host miR155 Promotes Tumor Growth through a Myeloid-Derived Suppressor Cell–Dependent Mechanism. *Cancer Research*, *75*(3), 519–531. https://doi.org/10.1158/0008-5472.CAN-14-2331

5. Datta, M., Coussens, L. M., Nishikawa, H., Hodi, F. S., & Jain, R. K. (2019). Reprogramming the Tumor Microenvironment to Improve Immunotherapy: Emerging Strategies and Combination Therapies. *American Society of Clinical Oncology Educational Book*, *39*, 165–174. https://doi.org/10.1200/EDBK_237987

6. DeNardo, D. G., & Ruffell, B. (2019). Macrophages as regulators of tumour immunity and immunotherapy. *Nature Reviews Immunology*, *19*(6), 369–382. https://doi.org/10.1038/s41577-019-0127-6

7. Duan, Q., Zhang, H., Zheng, J., & Zhang, L. (2020). Turning Cold into Hot: Firing up the Tumor Microenvironment. *Trends in Cancer*, *6*(7), 605–618. https://doi.org/10.1016/j.trecan.2020.02.022

8. Foster, S. L., Hargreaves, D. C., & Medzhitov, R. (2007). Gene-specific control of inflammation by TLR-induced chromatin modifications. *Nature*, *447*(7147), 972–978. https://doi.org/10.1038/nature05836

9. Fukumoto, T., Fatkhutdinov, N., Zundell, J. A., Tcyganov, E. N., Nacarelli, T., Karakashev, S., Wu, S., Liu, Q., Gabrilovich, D. I., & Zhang, R. (2019). HDAC6 Inhibition Synergizes with Anti-PD-L1 Therapy in ARID1A-Inactivated Ovarian Cancer. *Cancer Research*, *79*(21), 5482–5489. https://doi.org/10.1158/0008-5472.CAN-19-1302

10. Gatchalian, J., Liao, J., Maxwell, M. B., & Hargreaves, D. C. (2020). Control of Stimulus-Dependent Responses in Macrophages by SWI/SNF Chromatin Remodeling Complexes. *Trends in Immunology*, *41*(2), 126–140. https://doi.org/10.1016/j.it.2019.12.002

11. Gocher, A. M., Workman, C. J., & Vignali, D. A. A. (2022). Interferon-γ: Teammate or opponent in the tumour microenvironment? *Nature Reviews Immunology*, *22*(3), 158–172. https://doi.org/10.1038/s41577-021-00566-3

12. Gosselin, D., Skola, D., Coufal, N. G., Holtman, I. R., Schlachetzki, J. C. M., Sajti, E., Jaeger, B. N., O'Connor, C., Fitzpatrick, C., Pasillas, M. P., Pena, M., Adair, A., Gonda, D. D., Levy, M. L., Ransohoff, R. M., Gage, F. H., & Glass, C. K. (2017). An environment-dependent transcriptional network specifies human microglia identity. *Science*, *356*(6344), eaal3222. https://doi.org/10.1126/science.aal3222

13. Guha, P., Heatherton, K. R., O'Connell, K. P., Alexander, I. S., & Katz, S. C. (2022). Assessing the Future of Solid Tumor Immunotherapy. *Biomedicines*, *10*(3), 655. https://doi.org/10.3390/biomedicines10030655

14. Han, L., Madan, V., Mayakonda, A., Dakle, P., Woon, T. W., Shyamsunder, P., Nordin, H. B. M., Cao, Z., Sundaresan, J., Lei, I., Wang, Z., & Koeffler, H. P. (2019). Chromatin remodeling mediated by ARID1A is indispensable for normal hematopoiesis in mice. *Leukemia*, *33*(9), 2291–2305. https://doi.org/10.1038/s41375-019-0438-4

15. Hanahan, D., & Weinberg, R. A. (2000). The Hallmarks of Cancer. *Cell*, *100*(1), 57–70. https://doi.org/10.1016/S0092-8674(00)81683-9

16. Hegde, P. S., & Chen, D. S. (2020). Top 10 Challenges in Cancer Immunotherapy. *Immunity*, *52*(1), 17–35. https://doi.org/10.1016/j.immuni.2019.12.011

17. Jiménez-Uribe, A. P., Valencia-Martínez, H., Carballo-Uicab, G., Vallejo-Castillo, L., Medina-Rivero, E., Chacón-Salinas, R., Pavón, L., Velasco-Velázquez, M. A., Mellado-Sánchez, G., Estrada-Parra, S., & Pérez-Tapia, S. M. (2019). CD80 Expression Correlates with IL-6 Production in THP-1-Like Macrophages Costimulated with LPS and Dialyzable Leukocyte Extract (Transferon®). *Journal of Immunology Research*, *2019*, 1–9. https://doi.org/10.1155/2019/2198508

18. Krasteva, V., Crabtree, G. R., & Lessard, J. A. (2017). The BAF45a/PHF10 subunit of SWI/SNF-like chromatin remodeling complexes is essential for hematopoietic stem cell maintenance. *Experimental Hematology*, *48*, 58-71.e15. https://doi.org/10.1016/j.exphem.2016.11.008

19. Lecoultre, M., Dutoit, V., & Walker, P. R. (2020). Phagocytic function of tumor-associated macrophages as a key determinant of tumor progression control: A review. *Journal for ImmunoTherapy of Cancer*, *8*(2), e001408. https://doi.org/10.1136/jitc-2020-001408

20. Lewis, B. W., Patial, S., & Saini, Y. (2022). In Vitro Screening Method for Characterization of Macrophage Activation Responses. *Methods and Protocols*, *5*(5), 68. https://doi.org/10.3390/mps5050068

21. Lin, H., Wei, S., Hurt, E. M., Green, M. D., Zhao, L., Vatan, L., Szeliga, W., Herbst, R., Harms, P. W., Fecher, L. A., Vats, P., Chinnaiyan, A. M., Lao, C. D., Lawrence, T. S., Wicha, M., Hamanishi, J., Mandai, M., Kryczek, I., & Zou, W. (2018). Host expression of PD-L1 determines efficacy of PD-L1 pathway blockade–mediated tumor regression. *Journal of Clinical Investigation*, *128*(2), 805–815. https://doi.org/10.1172/JCI96113

22. Liu, Y., Carlsson, R., Ambjorn, M., Hasan, M., Badn, W., Darabi, A., Siesjo, P., & Issazadeh-Navikas, S. (2013). PD-L1 Expression by Neurons Nearby Tumors Indicates Better Prognosis in Glioblastoma Patients. *Journal of Neuroscience*, *33*(35), 14231–14245. https://doi.org/10.1523/JNEUROSCI.5812-12.2013

23. Mao, T.-L., & Shih, I.-M. (2013). The roles of ARID1A in gynecologic cancer. *Journal of Gynecologic Oncology*, *24*(4), 376. https://doi.org/10.3802/jgo.2013.24.4.376

24. Mas Martin, G., Man, N., Karl, D., Martinez, C., Duffort, S., Itonaga, H., Mookhtiar, A. K., Bilbao, D., Kunkalla, K., Valencia, A. M., Collings, C., Kadoch, C., Vega, F., Kogan, S. C., & Nimer, S. (2020). The Baf Subunit Dpf2 Regulates Resolution of Inflammation By Controlling Macrophage Differentiation Transcription Factor Networks. *Blood*, *136*(Supplement 1), 13–13. https://doi.org/10.1182/blood-2020-142030

25. Mellman, I., Coukos, G., & Dranoff, G. (2011). Cancer immunotherapy comes of age. *Nature*, *480*(7378), 480–489. https://doi.org/10.1038/nature10673

26. Morris, R., Kershaw, N. J., & Babon, J. J. (2018). The molecular details of cytokine signaling via the JAK/STAT pathway: Cytokine Signaling via the JAK/STAT Pathway. *Protein Science*, *27*(12), 1984–2009. https://doi.org/10.1002/pro.3519

27. Neophytou, C. M., Panagi, M., Stylianopoulos, T., & Papageorgis, P. (2021). The Role of Tumor Microenvironment in Cancer Metastasis: Molecular Mechanisms and Therapeutic Opportunities. *Cancers*, *13*(9), 2053. https://doi.org/10.3390/cancers13092053

28. Nixon, N. A., Blais, N., Ernst, S., Kollmannsberger, C., Bebb, G., Butler, M., Smylie, M., & Verma, S. (2018). Current Landscape of Immunotherapy in the Treatment of Solid Tumours, with Future Opportunities and Challenges. *Current Oncology*, *25*(5), 373–384. https://doi.org/10.3747/co.25.3840

29. Park, K., Veena, M. S., & Shin, D. S. (2022). Key Players of the Immunosuppressive Tumor Microenvironment and Emerging Therapeutic Strategies. *Frontiers in Cell and Developmental Biology*, *10*, 830208. https://doi.org/10.3389/fcell.2022.830208

30. Siegel, R. L., Miller, K. D., Fuchs, H. E., & Jemal, A. (2022). Cancer statistics, 2022. *CA: A Cancer Journal for Clinicians*, *72*(1), 7–33. https://doi.org/10.3322/caac.21708

31. Swartz, M. A., Iida, N., Roberts, E. W., Sangaletti, S., Wong, M. H., Yull, F. E., Coussens, L. M., & DeClerck, Y. A. (2012). Tumor Microenvironment Complexity: Emerging Roles in Cancer Therapy. *Cancer Research*, *72*(10), 2473–2480. https://doi.org/10.1158/0008-5472.CAN-12-0122

32. Tan, S., Li, D., & Zhu, X. (2020). Cancer immunotherapy: Pros, cons and beyond. *Biomedicine & Pharmacotherapy*, *124*, 109821. https://doi.org/10.1016/j.biopha.2020.109821

33. Xie, C., Liu, C., Wu, B., Lin, Y., Ma, T., Xiong, H., Wang, Q., Li, Z., Ma, C., & Tu, Z. (2016). Effects of IRF1 and IFN-β interaction on the M1 polarization of macrophages and its antitumor function. *International Journal of Molecular Medicine*, *38*(1), 148–160. https://doi.org/10.3892/ijmm.2016.2583

34. Zhang, W., Liu, Y., Yan, Z., Yang, H., Sun, W., Yao, Y., Chen, Y., & Jiang, R. (2020). IL-6 promotes PD-L1 expression in monocytes and macrophages by decreasing protein tyrosine phosphatase receptor type O expression in human hepatocellular carcinoma. *Journal for ImmunoTherapy of Cancer*, *8*(1), e000285. https://doi.org/10.1136/jitc-2019-000285

35. Zhou, Y., Fei, M., Zhang, G., Liang, W.-C., Lin, W., Wu, Y., Piskol, R., Ridgway, J., McNamara, E., Huang, H., Zhang, J., Oh, J., Patel, J. M., Jakubiak, D., Lau, J., Blackwood, B., Bravo, D. D., Shi, Y., Wang, J., … Yan, M. (2020). Blockade of the Phagocytic Receptor MerTK on Tumor-Associated Macrophages Enhances P2X7R-Dependent STING Activation by Tumor-Derived cGAMP. *Immunity*, *52*(2), 357-373.e9. https://doi.org/10.1016/j.immuni.2020.01.014